

New Dirhenium(III) Compounds Bridged by Carboxylate Ligands: N(C₄H₉)₄[Re₂(OOCFF₃)Cl₆] and Re₂(OOCCHCo₂(CO)₆)₄Cl₂

Andrés Vega,^{†,‡} Víctor Calvo,^{*,†} Jorge Manzur,[§] Evgenia Spodine,^{*,†} and Jean-Yves Saillard^{*,‡}

Facultad de Ciencias Químicas y Farmacéuticas, Centro para la Investigación Interdisciplinaria Avanzada en Ciencia de los Materiales, Universidad de Chile, Casilla 233, Santiago, Chile, Facultad de Ciencias Físicas y Matemáticas, Universidad de Chile, Casilla 2777, Santiago, Chile, and Laboratoire de Chimie du Solide et Inorganique Moléculaire, UMR-CNRS 6511, Institut de Chimie de Rennes, Université de Rennes 1, 35042 Rennes Cedex, France

Received March 26, 2002

The solvothermal reaction of N(C₄H₉)₄[Re₂Cl₈] with trifluoroacetic acid and acetic anhydride leads to the new rhenium trifluoroacetate dimer N(C₄H₉)₄[Re₂(OOCFF₃)Cl₆] (**1**) and to the rhenium carbonyl dimer Re₂(μ₂-Cl)₂(CO)₈ as the rhenium-reduced byproduct. The reaction of the precursor complex, N(C₄H₉)₄[Re₂(OOCFF₃)Cl₆] (**1**), with the organometallic carboxylic acid (CO)₆Co₂HCCCCOOH leads to the cluster of clusters compound Re₂(OOCCHCo₂(CO)₆)₄-Cl₂ (**2**), which has the dimer structure of Re₂(OOCR)₄Cl₂. Cyclic voltammetric measurements show that Re₂(OOCCHCo₂(CO)₆)₄Cl₂ (**2**) has one reduction centered on the dirhenium core and a reduction centered on the cobalt atoms. DFT calculations have been used to rationalize the observed displacements of the voltammetric signals in Re₂(OOCCHCo₂(CO)₆)₄Cl₂ (**2**) compared to the parent ligand (CO)₆Co₂HCCCCOOH and rhenium pivalate.

Introduction

There is considerable interest in the use of bimetallic units as the anchorage points for the construction of polymetallic or supramolecular entities.¹ The use of functionalized organometallic building blocks which can be coordinated to metal centers permits a new and versatile approach for the synthesis of high metal content compounds. This approach to polymetallic compounds is very attractive. Functionalized organometallic carboxylates have been used as blocks, taking advantage of the well-known carboxylate chemistry, to assemble more complex molecules with new properties. A striking example is that observed in systems such as M₂-(OOCOC₃(CO)₉)₄(OC₄H₈)₂ (M = Cr, Mo, W), where the organic carboxylate allows the electronic interaction between the inorganic coordinated fragment and the organometallic unit,² leading to polymetallic compounds with properties that are absent in the “simple” carboxylates, i.e., a low energy charge-transfer band from the quadruple bond to the cobalt

carbonyl fragment (at 300 nm for Cr, 536 nm for Mo, and 800 nm for W; ε ~ 35 000 cm⁻¹ M⁻¹).^{2,3} Moreover, the reactivity of an organocobalt carboxylic acid has been shown to be different from that of a simple one, as we recently described for the reaction of (CO)₆Co₂HCCCCOOH⁴ with copper(II) methoxide, which led to Cu₃(CCHCo₂(CO)₆)₃ instead of Cu(II) carboxylate.⁵

On the other hand, the success of this synthetic approach depends on the availability of an adequate metallic precursor. Mixed-ligand molybdenum complexes, like Mo₂(DANIF)₂-(MeCN)₄(BF₄)₂ (DANIF = *N,N'*-di-*p*-anisylformamidinate),⁶ or Re(CO)₅Cl⁷ appear to be adequate for supramolecular synthesis, exploiting some differences in the reactivity of the ligands. Metal carboxylates such as acetate or trifluoroacetate are known to be useful as precursors of polymetallic compounds.⁸

In this paper we describe the synthesis and structure of a new rhenium trifluoroacetate compound, N(C₄H₉)₄[Re₂-

* To whom correspondence should be addressed. E-mail: vcalvo@uchile.cl (V.C.); posgrado@uchile.cl (E.S.); saillard@univ-rennes1.fr (J.-Y.S.).

[†] Facultad de Ciencias Químicas y Farmacéuticas, Universidad de Chile.

[‡] Université de Rennes 1.

[§] Facultad de Ciencias Físicas y Matemáticas, Universidad de Chile.

(1) (a) Clérac, R.; Cotton, F. A.; Dunbar, K. R.; Murillo, C. A.; Wang, X. *Inorg. Chem.* **2001**, *40*, 420. (b) Cotton, F. A.; Donahue, J. P.; Lin, Ch.; Murillo, C. A. *Inorg. Chem.* **2001**, *40*, 1234. (c) Siewers, G. F.; Malafetse, T. J. *Chem. Rev.* **2000**, *100*, 853.

(2) Fehlner, T. P.; Calvo, V.; Cen, W. *J. Electron Spectrosc.* **1996**, *66*, 7289.

(3) Cen, W.; Lindenfeld, P.; Fehlner, T. P. *J. Am. Chem. Soc.* **1992**, *114*, 5451.

(4) Calvo, V.; Vega, A.; Cortes, P.; Spodine, E. *Inorg. Chim. Acta* **2002**, *333*, 15.

(5) Vega, A.; Calvo, V.; Spodine, E.; Zarate, A.; Fuenzalida, V.; Saillard, J.-Y. *Inorg. Chem.* **2002**, *41*, 0000.

(6) (a) Cotton, F. A.; Lin, C.; Murillo, C. A. *J. Chem. Soc., Dalton Trans.* **1998**, 3151. (b) Cotton, F. A.; Daniels, L.; Jordan, G., IV; Lin, C.; Murillo, C. A. *J. Am. Chem. Soc.* **1998**, *120*, 3398.

(OOCF₃)Cl₆] (1), suitable to be used as precursor for the synthesis of more complex rhenium species. A new rhenium organometallic carboxylate, Re₂(OOCCHCO₂(CO)₆)₄Cl₂ (2), prepared from 1, is structurally characterized and its electrochemistry studied. The existence of electronic interactions between the cobalt carbonyl peripheral fragments and the central dirhenium core in this compound is analyzed. Finally, we rationalize the effects of the organometallic cobalt carbonyl on the properties of the Re₂(OOCR₄)Cl₂ system by means of DFT calculations.

Experimental Section

(CO)₆Co₂HCCCOOH, [N(C₄H₉)₄]₂[Re₂Cl₈], and Re₂(OOC(CH₃)₃)₄Cl₂ were prepared according to literature methods.^{4,9,10} Tetrabutylammonium hexafluorophosphate, trifluoroacetic acid, and trifluoroacetic anhydride were purchased from Aldrich and used without further purification.

Syntheses. To find a rhenium precursor as a general starting point for the syntheses of hetero-polynuclear compounds, such as Re₂(OOCCHCO₂(CO)₆)₄Cl₂ (2), we made some attempts to prepare rhenium(III) trifluoroacetate. Trifluoroacetate salts are known to perform well as synthetic precursors,⁵ basically by their solubility in low-polarity organic solvents, where organometallic carboxylic acids such as (CO)₆Co₂HCCCOOH are stable.⁶ Attempts to prepare the starting material by refluxing octachlorodirhenate with trifluoroacetic acid and trifluoroacetic anhydride were unsuccessful. This was not completely surprising, owing to the relatively low boiling point of the trifluoroacetic mixture. Therefore, a more drastic approach was adopted, in which the reaction was carried out in a closed autogenous pressure reactor, to give N(C₄H₉)₄[Re₂(OOCF₃)Cl₆] (1) and the rhenium(I) carbonyl dimer Re₂(μ₂-Cl)₂(CO)₈¹¹ as a byproduct.

Solvothermal Preparation of N(C₄H₉)₄[Re₂(OOCF₃)Cl₆] (1). A 2.0 g amount of [N(C₄H₉)₄]₂[Re₂Cl₈], 4 mL of trifluoroacetic acid, and 0.2 mL of trifluoroacetic anhydride were mixed in a Parr vessel. Two reaction temperatures, 180 and 250 °C, were tried, and a heating time of 48 h was used. The reaction vessel was open after cooling to room temperature. A solid with only a residual quantity of liquid was obtained as the raw product of the reaction. Treatment of this product with acetone allows the isolation of a semitransparent solid which is insoluble. Single-crystal X-ray, IR, and elemental analyses showed that this solid corresponds to Re₂(μ₂-Cl)₂(CO)₈.¹¹ The yield of this product (estimated by weighing the insoluble residue after extraction with acetone) based on rhenium content is about 30% at 250 °C and diminishes to about 8% at 180 °C. No attempts were made to fully investigate if this collateral reaction disappears at lower temperatures or for shorter reaction times. Compound 1 can be isolated as brown crystals by careful separation of the crude reaction product under a microscope or as a microcrystalline powder after filtering and cooling the acetone

Table 1. Summary of Crystal Data and Refinement Details for N(C₄H₉)₄[Re₂(OOCF₃)Cl₆] (1) and Re₂(OOCCHCO₂(CO)₆)₄Cl₂ (2)

param	1	2
formula	C ₁₈ H ₃₆ Cl ₆ F ₃ NO ₂ Re ₂	C ₃₆ H ₄ Cl ₂ Co ₈ O ₃₂ Re ₂
mol wt	940.6	1863.1
cryst syst	monoclinic	monoclinic
space group	<i>P</i> 2 ₁ / <i>n</i>	<i>P</i> 2 ₁ / <i>c</i>
<i>a</i> , Å	12.3006(7)	10.215(3)
<i>b</i> , Å	15.1612(8)	25.640(7)
<i>c</i> , Å	16.447(1)	10.474(3)
β, deg	95.296(1)	96.36(2)
<i>V</i> , Å ³	3054.1(3)	2726(1)
<i>Z</i>	4	2
<i>D</i> _c , kg m ⁻³	2.046	2.269
<i>F</i> (000)	1784	1752
μ(Mo Kα), mm ⁻¹	8.479	6.976
<i>R</i> ^a	0.0433	0.0450
<i>R</i> _w ^b	0.1137	0.0696

^a $R = \sum ||F_o| - |F_c|| / \sum |F_o|$. ^b $R_w = [\sum [w(F_o^2 - F_c^2)^2] / \sum [w(F_o^2)^2]]^{1/2}$. *T* = 25 °C.

extract or by vacuum evaporation of the solvent. IR spectra and elemental analysis of the powder and the crystalline material showed no significant differences. The structure of 1 was determined by X-ray diffraction on a crystal directly taken from the synthesis vessel.

Anal. Calcd for N(C₄H₉)₄[Re₂(OOCF₃)Cl₆] (1): C, 22.98; H, 3.86; N, 1.49; Re, 39.59. Found: C, 23.1; H, 4.0; N, 1.6; Re, 39.1.

IR (KBr pellet) ($\nu_{\max}/\text{cm}^{-1}$): 2965 (m), 2932 (m), 2875 (m), 1684 (s), 1597 (m), 1466 (s), 2382 (s), 1204 (vs), 1157 (vs), 925 (s).

Synthesis of Re₂(OOCCHCO₂(CO)₆)₄Cl₂ (2). This compound was prepared by reaction of the rhenium precursor 1 (either as crystalline or powder material) with (CO)₆Co₂HCCCOOH, using standard Schlenk techniques. Stoichiometric quantities of 1 and (CO)₆Co₂HCCCOOH were dissolved in freshly distilled CH₂Cl₂. The (CO)₆Co₂HCCCOOH solution was slowly added to the rhenium precursor solution. The resulting mixture was stirred for a 4 h period. Then the solvent was completely evaporated under vacuum. The solid product was then extracted with CH₂Cl₂ and filtered through activated silica. After volume reduction the extract was allowed to stand at low temperature (0 °C). X-ray-quality, brownish red crystals were formed from the solution after 3 days.

Anal. Calcd for Re₂(OOCCHCO₂(CO)₆)₄Cl₂ (2): C, 23.21; H, 0.74; Re, 19.99; Co, 25.31. Found: C, 23.43; H, 0.74; Re, 19.40; Co, 24.9.

IR (KBr pellet) ($\nu_{\max}/\text{cm}^{-1}$): ν_{CO} (terminal), 2113 (s), 2057 (s), 2005 (s); ν_{COO} , 1540 (m), 1415 (m), 1326 (m).

Measurements and Analyses. IR spectra were recorded in KBr pellets on a Vector 22 spectrophotometer. Elemental and metal content analyses were done at CEPEDEQ, Universidad de Chile.

X-ray diffraction. N(C₄H₉)₄[Re₂(OOCF₃)Cl₆] (1). A 0.3 × 0.4 × 0.6 mm brown crystal of the rhenium mono(trifluoroacetate) (1) (taken directly from the synthesis vessel) was mounted on a glass fiber. Data collection was made on a Bruker SMART APEX diffractometer, using 0.3° of separation between frames. Data integration was made using SAINT.¹² Semiempirical absorption corrections were applied using SADABS¹² ($T_{\min} = 0.31$, $T_{\max} = 0.95$). The structure was solved using XS in SHELXTL¹³ by means of direct methods and completed by Fourier difference synthesis. Refinement until convergence was achieved using XL SHELXTL.¹³ For additional data collection and refinement details, see Table 1.

(12) SADABS: Area-Detector Absorption Correction; Siemens Industrial Automation, Inc.: Madison, WI, 1998.

(13) Sheldrick, G. M. SHELXTL V 5.1; Bruker AXS: Madison, WI, 1998.

(7) Slone, R. V.; Hupp, J. T.; Sternm, C. L.; Albrecht-Schmitt, T. E. *Inorg. Chem.* **1996**, *35*, 4096.

(8) (a) Calvo, V.; Fehlner, T. P.; Rheingold, A. L. *Inorg. Chem.* **1996**, *35*, 7289. (b) Calvo, V.; Shang, M.; Yap, G.; Rheingold, A.; Fehlner, T. P. *Polyhedron* **1999**, *18*, 1869. (c) Cotton, F. A.; Dikarev, E. V.; Petrukhina, M. A.; Schmitz, M.; Stang, P. J. *Inorg. Chem.* **2002**, *41*, 2903.

(9) Cotton, F. A.; Curtis, N. F.; Johnson, B. F. G.; Robinson, W. R. *Inorg. Chem.* **1965**, *4*, 330.

(10) Cotton, F. A.; Oldham, C.; Robinson, W. R. *Inorg. Chem.* **1966**, *5*, 1798.

(11) Pasynskii, A. A.; Shaposhnikova, A. D.; Zalmanovich, Y. V.; Ermenko, I. L.; Antsyshkina, A. S.; Belskii, V. K. *Koord. Khim.* **1985**, *11*, 988.

$\text{Re}_2(\text{OCCCC}(\text{CO})_2)_4\text{Cl}_2$ (**2**). A $0.4 \times 0.5 \times 0.1$ mm red crystal was mounted on a glass fiber at room temperature. Preliminary examination and data collection showed acceptable crystal quality. Cell parameters were calculated from 25 reflections. Data set was collected between 3.18 and 50.00° in the 2θ angle on a Siemens R3m diffractometer. Lorentz and polarization corrections were incorporated in data reduction using XDISK.¹⁴ Semiempirical ψ -scan absorption corrections were applied, using XPREP ($T_{\min} = 0.38$, $T_{\max} = 0.79$). The structure was solved using direct methods in XS, completed by Fourier difference synthesis, and refined using XL in SHELXTL/PC.¹⁵ Hydrogen atoms were also located by difference Fourier synthesis and refined in subsequent least-squares cycles, with the C–H distance restricted to be 1.00 \AA (free to refine parameter). For more details about data collection and refinement, see Table 1.

Cyclic Voltammetry. Cyclic voltammograms for **2** and $\text{Re}_2(\text{OCC}(\text{CH}_3)_3)_4\text{Cl}_2$ were recorded in CH_2Cl_2 solutions (0.5×10^{-4} M) using tetrabutylammonium hexafluorophosphate (0.1 M) as supporting electrolyte. Cyclic voltammograms were recorded at various sweep rates: 50 , 100 , 200 , 300 , 400 , and 500 mV s^{-1} . A vitreous carbon electrode was used as working electrode, a platinum electrode was used as auxiliary electrode, and a saturated calomel electrode was used as reference electrode.

Computational Details. DFT¹⁶ calculations were carried out using the Amsterdam Density Functional (ADF) program.¹⁷ The Vosko–Wilk–Nusair parametrization¹⁸ was used for the local density approximation with gradient corrections for exchange (Becke88)¹⁹ and correlation (Perdew)²⁰ (BP), respectively. The numerical integration procedure applied for the calculation was developed by te Velde.^{16d} Relativistic corrections were added by the use of the ZORA (zeroth order regular approximation) scalar Hamiltonian.²¹ A double- ζ STO basis set was employed for H 1s, C, N 2s and 2p, and Cl 3s and 3p extended with a single- ζ polarization 2p function for H, 3d for C and N, and for Cl 4d. A triple- ζ STO basis set was used for Co 3d and 4s, extended with a single- ζ polarization for Co 4p. A double- ζ STO basis set was used for Re 5s, and a triple- ζ STO basis set was used for Re 4f, 5p, 5d, and 6s extended with a single polarization function for 6p. Full geometry optimizations were carried out on each complex using the analytical gradient method implemented by Verluis and Ziegler.²² No symmetry constraint was used in the geometry optimization of $(\text{CO})_6\text{Co}_2\text{HCCCCOOH}$ and its anion. C_{4h} symmetry is the highest possible symmetry to model **2**. However, since the ADF2000 version used for the calculations does not recognize this symmetry, C_{2h} symmetry was used for optimizations on $\{\text{Re}_2(\text{OCC}(\text{CH}_3)_3)_4\text{Cl}_2\}^{0/-}$ and **2**. No significant deviation from C_{4h} symmetry was found in the optimized geometries. The geometry of 2^- was

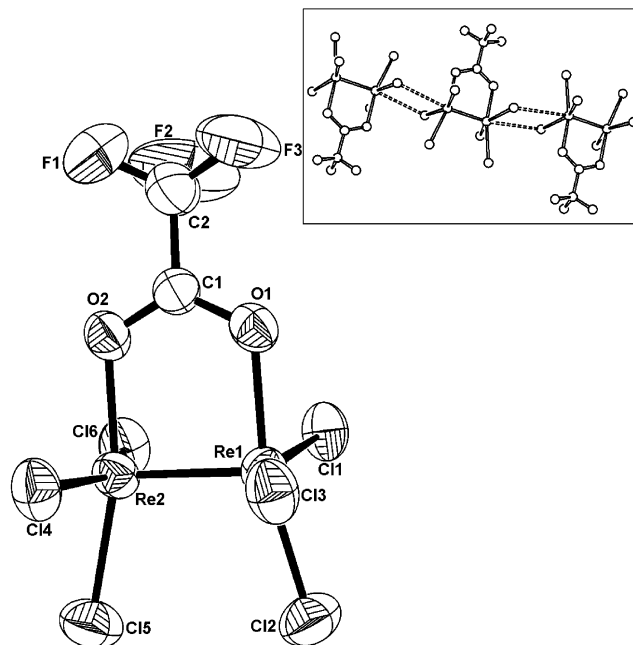


Figure 1. X-ray molecular structure of the dirhenium mono(trifluoroacetate) anion in **1**. Insert: Packing scheme showing intermolecular contacts.

not optimized, and a single point calculation was done using the computed geometry of **2**. Spin unrestricted calculations were done for all the odd-electron systems.

Results and Discussion

(a) Structural Analysis. The rhenium carbonyl byproduct $\text{Re}_2(\mu_2\text{-Cl})_2(\text{CO})_8$ has been fully characterized by single-crystal X-ray diffraction. Since its molecular structure has been already published,¹¹ it is not described here (see Supporting Information). This carbonyl consists of two $\text{Re}(\text{CO})_4$ units bridged by two chloride ions, defining a Re_2Cl_2 central parallelogram.

Figure 1 shows the X-ray molecular structure of the anion of compound **1**. Selected bond distances and angles are given in Table 2. The $[\text{Re}_2(\text{OCCF}_3)\text{Cl}_6]^-$ anion in **1** has a central Re–Re motif, with a distance of $2.2361(5) \text{ \AA}$, as typically described for quadruply bonded rhenium atoms.²³ There are contacts between the chloride ions in the $[\text{Re}_2(\text{OCCF}_3)\text{Cl}_6]^-$ motif and the axial position of a rhenium atom in a symmetry-related unit, in such a way that linear chains of anionic units surrounded by ammonium cations are formed (see insert in Figure 1). The values for this axial contacts are 2.921 \AA ($\text{Re}2 \cdots \text{Cl}4$, $2 - x, 1 - y, 2 - z$) and 3.166 \AA ($\text{Re}1 \cdots \text{Cl}1$, $1 - x, 1 - y, 2 - z$). This complex is, to the best of our knowledge, the first dirhenium(III) mono(trifluoroacetate) compound structurally determined, in which the carboxylate bridges the two 16-electron metal centers. At the same time, it represents the first example of a monocarboxylate hexachloride compound of the Re_2^{6+} unit. Other examples of this kind of substitution on the octachlorodirhenate ion are limited to phosphines²⁴ and amides²⁵ but not to carboxylate bridges. The Cambridge Structural Da-

(14) *P3-P4/PC, Version 4.2*; Siemens Analytical X-ray Instruments Inc.: Madison, WI, 1991.

(15) Sheldrick, G. M. *SHELXTL version 5.0*; Siemens Analytical X-ray Instruments Inc.: Madison, WI, 1993.

(16) (a) Baerends, E. J.; Ellis, D. E.; Ros, P. *Chem. Phys.* **1973**, *2*, 41. (b) Baerends, E. J.; Ros, P. *Int. J. Quantum Chem.* **1978**, *S12*, 169. (c) Boerrigter, P. M.; te Velde, G.; Baerends, E. J. *Int. J. Quantum Chem.* **1988**, *33*, 87. (d) te Velde, G.; Baerends, E. J. *J. Comput. Phys.* **1992**, *99*, 84.

(17) *Amsterdam Density Functional (ADF) program, version 2000*; Vrije Universiteit: Amsterdam, The Netherlands, 2000.

(18) Vosko, S. D.; Wilk, L.; Nusair, M. *Can. J. Chem.* **1990**, *58*, 1200.

(19) (a) Becke, A. D. *J. Chem. Phys.* **1986**, *84*, 4524. (b) Becke, A. D. *Phys. Rev. A* **1988**, *38*, 2098.

(20) (a) Perdew, J. P. *Phys. Rev. B* **1986**, *33*, 8882. (b) Perdew, J. P. *Phys. Rev. B* **1986**, *34*, 7406.

(21) (a) van Lenthe, E.; Baerends, E. J.; Snijders, J. G. *J. Chem. Phys.* **1993**, *99*, 4597. (b) van Lenthe, E.; Baerends, E. J.; Snijders, J. G. *J. Chem. Phys.* **1994**, *101*, 9783. (c) van Lenthe, E.; van Leeuwen, R.; Baerends, E. J. *Int. J. Quantum Chem.* **1996**, *57*, 281.

(22) Verluis, L.; Ziegler, T. *J. Chem. Phys.* **1988**, *88*, 322.

(23) Cotton, F. A.; Walton, R. A. *Multiple Bonds Between Metal Atoms*, 2nd ed.; Clarendon Press: Oxford, U.K., 1993.

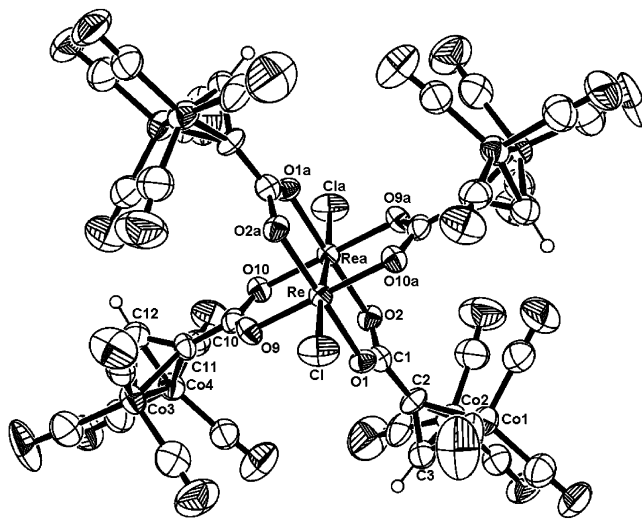
Table 2. Selected Bond Distances (Å) and Angles and Torsion Angles (deg) for $N(C_4H_9)_4[Re_2(OOCCF_3)Cl_6]$ (**1**) and $Re_2(OOCCCHCo_2(CO)_6)_4Cl_2$ (**2**)

$N(C_4H_9)_4[Re_2(OOCCF_3)Cl_6]$ (1)			
Re(1)–O(1)	2.078(5)	Re(2)–O(2)	2.065(5)
Re(1)–Cl(1)	2.314(2)	Re(2)–Cl(4)	2.347(2)
Re(1)–Cl(2)	2.279(2)	Re(2)–Cl(5)	2.278(2)
Re(1)–Cl(3)	2.305(2)	Re(2)–Cl(6)	2.310(2)
C(1)–O(1)	1.260(8)	C(1)–O(2)	1.244(7)
Re(1)–Re(2)	2.2361(5)		
Cl(2)–Re(1)–Cl(3)	90.68(8)	Cl(2)–Re(1)–Cl(1)	90.70(8)
Cl(3)–Re(1)–Cl(1)	151.25(7)	Cl(5)–Re(2)–Cl(6)	91.19(8)
Cl(5)–Re(2)–Cl(4)	90.47(8)	Cl(6)–Re(2)–Cl(4)	155.56(7)
C(1)–O(1)–Re(1)	117.4(4)	C(1)–O(2)–Re(2)	118.9(4)
O(2)–C(1)–O(1)	124.1(7)	O(2)–C(1)–C(2)	118.0(7)
O(1)–C(1)–C(2)	117.9(6)		
$Re_2(OOCCCHCo_2(CO)_6)_4Cl_2$ (2)			
Re–Re(a)	2.240(1)	Re–Cl	2.473(3)
Re–O(1)	2.025(6)	Re–O(9)	2.035(6)
Re–O(2a)	2.010(6)	Re–O(10a)	2.036(6)
O(1)–C(1)	1.27(1)	O(9)–C(10)	1.29(1)
C(1)–O(2)	1.30(1)	C(10)–O(10)	1.26(1)
C(1)–C(2)	1.44(1)	C(10)–C(11)	1.45(1)
C(2)–C(3)	1.34(1)	C(11)–C(12)	1.35(1)
Co(1)–Co(2)	2.483(2)	Co(3)–Co(4)	2.473(2)
O(1)–Re–O(9)	90.1(2)	O(1)–Re–O(10a)	90.7(2)
O(9)–Re–O(10a)	179.2(2)	O(2)–Re(a)–O(9)	89.9(2)
O(1)–Re–Cl	89.1(2)	O(9)–Re–Cl	94.1(2)
O(1)–C(1)–O(2)	120.8(8)	C(3)–C(2)–C(1)	142(1)
O(10)–C(10)–O(9)	122(1)	C(12)–C(11)–C(10)	145(1)
Re(a)–Re–Cl	174.83(8)		
O(1)–C(1)–C(2)–C(3)	61.3(18)	O(10)–C(10)–C(11)–C(12)	42(2)
O(2)–C(1)–C(2)–C(3)	119.6(14)	O(9)–C(10)–C(11)–C(12)	142.9(15)

^a $-x + 1, -y + 2, -z + 1$.

tabase²⁶ refers only one example of coordinated trifluoroacetate, the trinuclear rhenium(I) carbonyl compound $[N(C_2H_5)_4][Re_3(\mu_2-H)_3(CO)_{10}(\mu_2-OOCCF_3)]$.²⁷

Figure 2 shows the X-ray molecular structure for compound **2**. Table 2 shows selected bond distances and angles. It has a dirhenium central core surrounded by four bridging organometallic carboxylates and by terminal chlorides, an arrangement which is common to simple rhenium carboxylates.²³ The structure has a crystallographic inversion center in the middle of the rhenium–rhenium bond. The distance between the rhenium atoms is 2.240(1) Å, a value which is similar to the metal–metal distance in structurally related quadruply bonded compounds.²³ Although the $(CO)_6Co_2HCCCOOH$ ligand retains all its connectivity (a C_2Co_2 core with carbonyls, carboxylate, and hydrogen groups), when coordinated to rhenium in comparison to the acid, some subtle conformation differences between the observed structures for both (coordinated and uncoordinated) forms of

**Figure 2.** X-ray molecular structure of the cluster of clusters compound **2**.**Table 3.** Cyclic Voltammetry Parameters for $Re_2(OOCCCHCo_2(CO)_6)_4Cl_2$ (**2**), $(CO)_6Co_2HCCCOOH$, and $Re_2(OOCC(CH_3)_3)_4Cl_2$

compd	E_{pc}/mV	E_{pa}/mV	$\Delta E/mV$	i_{pa}/i_{pc}
$(CO)_6Co_2HCCCOOH^a$	–1015			
$Re_2(OOCC(CH_3)_3)_4Cl_2$	–507	–345	162	0.95
$Re_2(OOCCCHCo_2(CO)_6)_4Cl_2$ (2)	–365	–290	75	0.75
	–1086			

^a Reference 4.

$(CO)_6Co_2HCCCOO$ are observed. The angle defined by the carbon atoms of the HCCCOO fragment has an average value of 143° for **2**, which significantly deviates from the value of 129° observed in $(CO)_6Co_2HCCCOOH$.⁴ The dihedral angle defined by the carboxylate group (OCO plane) is nearly perpendicular to the plane defined by the carbon atoms in the organic acid fragment (CCC plane) in $(CO)_6Co_2HCCCOOH$ (94°),⁴ but for **2** the observed values are lower (40.1, 60.8°). The reason for that is likely to be of steric and/or packing origin. Indeed, the distance between carbon atoms in the C_2Co_2 (average 1.34 Å) core remains statistically the same, when compared with $(CO)_6Co_2HCCCOOH$ (1.32 Å).⁴

(b) Cyclic Voltammetry. The cyclic voltammogram of **2** shows two waves, one semireversible wave centered at –328 mV and a completely irreversible wave at –1086 mV. The corresponding oxidation peak for the first of these reductions is located at –290 mV. The i_{pa}/i_{pc} ratio for this signal is 0.75 and it is increased at higher sweep rates. The potential for this reduction process is shifted to less negative values with higher sweep rates, while the potential for the corresponding oxidation process becomes more positive as the sweep rate is increased. The second reduction process at –1086 mV is completely irreversible for all the sweep rates measured. The E_{pc} values for this signal are not too sensitive to the changes in sweep rates. There is another oxidation signal observed at 40 mV, which is related to decomposition of the compound during the reduction process, as demonstrated by partial sweep experiments. Table 3 shows a summary of the voltammetric parameters measured for **2**, in comparison with the values for $(CO)_6Co_2HCCCOOH$ and $Re_2(OOCC(CH_3)_3)_4Cl_2$.

- (24) (a) Cotton, F. A.; Foxman, B. M. *Inorg. Chem.* **1968**, *7*, 2135. (b) Cotton, F. A.; Diebold, M. P.; Roth, W. J. *Inorg. Chim. Acta* **1988**, *144*, 17. (c) Chen, J. D.; Cotton, F. A. *J. Am. Chem. Soc.* **1991**, *113*, 2509. (d) Cotton, F. A.; Dikarev, E. V.; Petrukhina, M. A. *J. Am. Chem. Soc.* **1997**, *119*, 12541. (e) Cotton, F. A.; Dikarev, E. V.; Petrukhina, M. A. *Inorg. Chem.* **1998**, *37*, 1949. (f) Cotton, F. A.; Dikarev, E. V.; Jordan, G. T., IV; Murillo, C. A.; Petrukhina, M. A. *Inorg. Chem.* **1998**, *37*, 4611.
- (25) (a) McGaff, R. W.; Dopke, N. C.; Hayashi, R. K.; Powell, D. R.; Treichel, P. M. *Polyhedron* **2000**, *19*, 1245. (b) Nelson, K. J.; McGaff, R. W.; Powell, D. R. *Inorg. Chim. Acta* **2000**, *304*, 130.
- (26) *Cambridge Structural Data Base*, version 5.20; Cambridge Crystallographic Data Center: Cambridge, United Kingdom, 2001.
- (27) Beringhelli, T.; Ciani, G.; D'Alfonso, G.; Sironi, A.; Freni, M. *J. Organomet. Chem.* **1982**, *233*, C46.

Table 4. X-ray and DFT-Optimized Metrical Parameters for $\{(\text{CO})_6\text{Co}_2\text{HCCCOOH}\}^{0/-}$, $\{\text{Re}_2(\text{O}(\text{OCC}(\text{CH}_3)_3)_4\text{Cl}_2)\}^{0/-}$, and **2**^a

dist (Å)	$(\text{CO})_6\text{Co}_2\text{HCCCOOH}$		$\{(\text{CO})_6\text{Co}_2\text{HCCCOOH}\}^-$	$\text{Re}_2(\text{O}(\text{OCC}(\text{CH}_3)_3)_4\text{Cl}_2)$		$\{\text{Re}_2(\text{O}(\text{OCC}(\text{CH}_3)_3)_4\text{Cl}_2)^-$	2
	X-ray ^a	DFT	DFT	X-ray ^c	DFT	DFT	DFT
Co–Co	2.483	2.524	2.860				2.522
C _{ac} –C _{cx}	1.49	1.472	1.455				1.467
C _{cx} –O	1.24–1.30	1.219–1.368	1.227–1.387				1.293
C _{ac} –C _{ac}	1.32	1.353	1.334				1.358
Co–C _{ac}	1.92	1.977	2.038				
Re–Re				2.236	2.262	2.264	2.289
Re–Cl				2.477	2.440	2.581	2.467
Re–O _{cx}				2.026	2.002	2.090	2.048

^a Some distances are averaged. C_{cx}: carboxylate carbon. C_{ac}: acetylenic carbon. O_{cx}: carboxylate oxygen. ^b Reference 4. ^c Reference 10.

Table 5. DFT Mulliken Charges for $\{(\text{CO})_6\text{Co}_2\text{HCCCOOH}\}^{0/-}$, $\{\text{Re}_2(\text{O}(\text{OCC}(\text{CH}_3)_3)_4\text{Cl}_2)\}^{0/-}$, and **2**^{0/-} ^a

atom	$(\text{CO})_6\text{Co}_2\text{HCCCOOH}$	$\{(\text{CO})_6\text{Co}_2\text{HCCCOOH}\}^-$	$\text{Re}_2[\text{O}(\text{OCC}(\text{CH}_3)_3)_4\text{Cl}_2]$	$\text{Re}_2[\text{O}(\text{OCC}(\text{CH}_3)_3)_4\text{Cl}_2]^-$	2	2 ⁻
Co	-0.57	-0.61 (0.47)			-0.15	-0.10 (0.06)
C _{cx}	0.77	0.75 (-0.01)	0.94	0.93 (-0.02)	0.83	0.84 (0.00)
Re			1.30	1.20 (0.49)	1.27	1.19 (0.27)
O _{cx}			-0.65	-0.67 (0.01)	-0.65	-0.67 (0.02)
Cl			-0.45	-0.60 (-0.01)	-0.41	-0.46 (-0.00)

^a Spin densities are shown in parentheses. C_{cx}: carboxylate carbon. O_{cx}: carboxylate oxygen.

Simple dirhenium carboxylates, like $\text{Re}_2(\text{O}(\text{OCC}(\text{CH}_3)_3)_4\text{Cl}_2)$, show a one-electron quasi-reversible reduction in many solvents.²⁸ The value of $E_{1/2}$ in dichloromethane solution for rhenium pivalate is -420 mV vs SCE.²⁸ Experimentally measured values for E_{pc} and E_{pa} for rhenium pivalate in this work, under a set of conditions similar to those for **2**, are -507 and -345 mV, respectively. These values can be well compared with the potential values for **2**, clearly suggesting that this redox process corresponds to the one-electron reduction of the compound, $\text{2}/\text{2}^-$, centered on the dirhenium core. The reduction wave at -1086 mV in the cyclic voltammogram of **2** can be assigned to the reduction of the cobalt fragments in the molecule. It has been demonstrated for $(\text{CO})_6\text{Co}_2\text{HCCCOOH}$ that the irreversible reduction wave observed at -1015 mV corresponds to the one-electron reduction of the organometallic acid.⁴ This process is common to most of the C_2Co_2 systems and is basically related to the cobalt carbonyl fragment.²⁹ Coordination of $(\text{CO})_6\text{Co}_2\text{HCCCOOH}$ to rhenium centers does not affect the nonreversibility of this process but shifts the potential to more negative values.

In this way, the cyclic voltammogram of **2** can be explained in terms of the redox processes arising from the dirhenium and the cobalt carbonyl fragments, but we must comment on the difference in the potential values between **2** and the corresponding values for $(\text{CO})_6\text{Co}_2\text{HCCCOOH}$ and $\text{Re}_2(\text{O}(\text{OCC}(\text{CH}_3)_3)_4\text{Cl}_2)$. When one compares the potential

value for the dirhenium reduction process, a 142 mV displacement in the E_{pc} is observed. Similarly, a 70 mV shift is observed for the reduction of the cobalt carbonyl fragment when it is coordinated to the dirhenium core. These shifts clearly suggest an interaction between the dirhenium core and the cobalt carbonyl fragments, as reflected by the change in the potential necessary for both reductions.

(c) Theoretical Investigation. To rationalize the electronic structure of **2** and to understand the underlying factors that govern the reduction potential shifts observed in cyclic voltammetry, we have carried out DFT calculations. Full geometry optimizations were carried out for $\{(\text{CO})_6\text{Co}_2\text{HCCCOOH}\}^{0/-}$, $\{\text{Re}_2(\text{O}(\text{OCC}(\text{CH}_3)_3)_4\text{Cl}_2)\}^{0/-}$, and **2**. Table 4 shows the major measured and computed geometrical parameters. In all cases there is a good agreement between the experimental X-ray distances and the optimized DFT geometries. Computed net charges and spin densities are given in Table 5 for $\{(\text{CO})_6\text{Co}_2\text{HCCCOOH}\}^{0/-}$, $\{\text{Re}_2(\text{O}(\text{OCC}(\text{CH}_3)_3)_4\text{Cl}_2)\}^{0/-}$, and $\text{2}^{0/-}$.

Figure 3 shows the simplified molecular orbital diagrams of $(\text{CO})_6\text{Co}_2\text{HCCCOOH}$, $\text{Re}_2(\text{O}(\text{OCC}(\text{CH}_3)_3)_4\text{Cl}_2)$ and **2**. As expected from the $\sigma_{\text{Co-Co}}^*$ antibonding character of the LUMO in $(\text{CO})_6\text{Co}_2\text{HCCCOOH}$, the addition of an extra electron leads to a lengthening of the Co–Co distance, which is consistent with the reported electrochemical irreversibility of this reduction process.⁴ On the other hand, the LUMO of $\text{Re}_2(\text{O}(\text{OCC}(\text{CH}_3)_3)_4\text{Cl}_2)$ is mainly localized on the central rhenium core with $\delta_{\text{Re-Re}}^*$ antibonding character. Consistently, the one-electron reduction of $\text{Re}_2(\text{O}(\text{OCC}(\text{CH}_3)_3)_4\text{Cl}_2)$ reduces the rhenium net charge. The spin density computed for $\{\text{Re}_2(\text{O}(\text{OCC}(\text{CH}_3)_3)_4\text{Cl}_2)\}^{0/-}$ confirms that the extra electron is mainly located on the dirhenium core (Table 5). The one-electron occupation of the $\delta_{\text{Re-Re}}^*$ orbital does not introduce appreciable geometrical changes in $\{\text{Re}_2(\text{O}(\text{OCC}(\text{CH}_3)_3)_4\text{Cl}_2)^-$ when compared to $\text{Re}_2(\text{O}(\text{OCC}(\text{CH}_3)_3)_4\text{Cl}_2)$ (see Table 4).

As commented in the voltammetric results, the electrochemical behavior of **2** can be understood in terms of a

(28) (a) Srinivasan, V.; Walton, R. A. *Inorg. Chem.* **1980**, *19*, 1635. (b) Cotton, F. A.; Pedersen, M. J. *Am. Chem. Soc.* **1975**, *97*, 303.

(29) (a) Bond, A. M.; Peake, B. M.; Robinson, B. H.; Simpson, J.; Watson, D. G. *Inorg. Chem.* **1977**, *16*, 41. (b) Osella, D.; Fiedler, J. *Organometallics* **1992**, *11*, 3875. (c) Aggarwal, R. P.; Connelly, N. G.; Crespo, M. C.; Dunne, B. J.; Hopkins, P.; Orpen, A. G. *J. Chem. Soc., Dalton. Trans.* **1992**, 655. (d) Lewis, J.; Lin, B.; Khan, M. S.; Al-Mandhary, M.; Raithby, P. R. *J. Organomet. Chem.* **1994**, *484*, 161. (e) Duffy, N.; McAdam, J.; Nervi, C.; Osella, D.; Ravera, M.; Robinson, B.; Simson, J. *Inorg. Chim. Acta* **1996**, *247*, 99. (f) McAdam, J.; Duffy, N. W.; Robinson, B.; Simpson, J. *J. Organomet. Chem.* **1997**, *527*, 179. (g) Low, P. J.; Rousseau, R.; Udachin, K. A.; Enright, G. D.; Tse, J. S.; Wayner, D.; Carty, A. *Organometallics* **1999**, *18*, 3885.

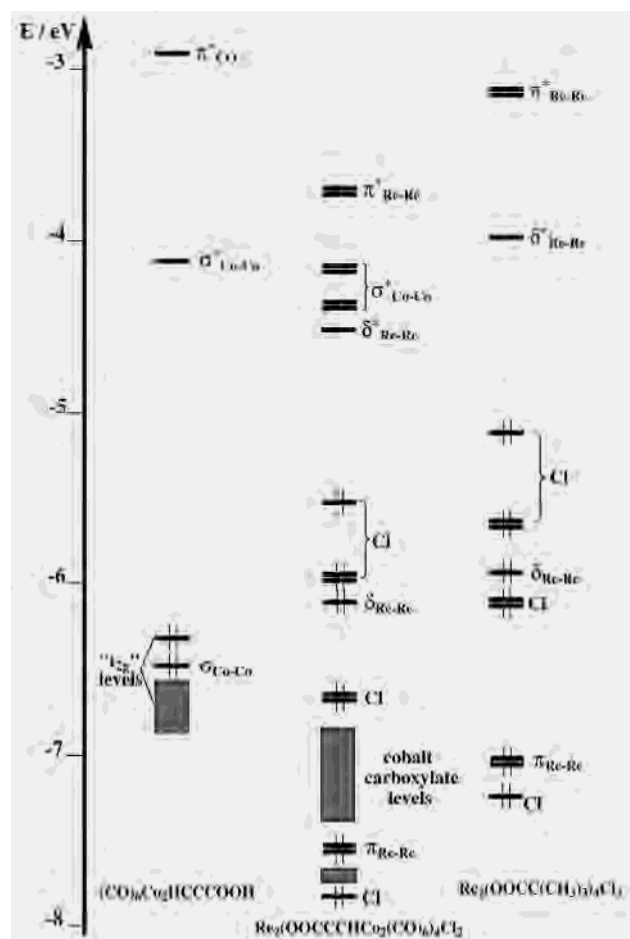


Figure 3. MO diagram of $(\text{CO})_6\text{Co}_2\text{HCCCOOH}$, $\text{Re}_2(\text{OOCC}(\text{CH}_3)_3)_4\text{Cl}_2$, and **2**.

reduction process related to the dirhenium core and the other one related to the cobalt–carbonyl peripheral system. This would be consistent with a LUMO mainly localized on the dirhenium core and a LUMO+1 related to the cobalt carbonyl fragments on the molecule. DFT results (Figure 3) show basically this scheme: a LUMO with $\delta^*_{\text{Re-Re}}$ character and just above four orbitals which can be identified as combinations of the four $\sigma^*_{\text{Co-Co}}$ orbitals. Surprisingly, the $\delta^*_{\text{Re-Re}}$ orbital shows no cobalt contribution and vice versa for the four $\sigma^*_{\text{Co-Co}}$ levels, contrary to what one can expect

from the displacements of the reduction waves in **2** as compared to $(\text{CO})_6\text{Co}_2\text{HCCCOOH}$ and $\text{Re}_2(\text{OOCC}(\text{CH}_3)_3)_4\text{Cl}_2$. Assuming that, as found for the $\{\text{Re}_2(\text{OOCC}(\text{CH}_3)_3)_4\text{Cl}_2\}^{0/-}$ system (see above), the one-electron reduction of **2** does not produce great geometrical changes, a single point calculation on **2**⁻ using the optimized geometry of **2** was carried out. It turns out that the electron relaxation associated with the addition of an extra electron to **2** causes significant mixing between the $\delta^*_{\text{Re-Re}}$ and the nearby $\sigma^*_{\text{Co-Co}}$ levels. This is reflected in a significantly lower spin density on the rhenium atoms as compared to $\{\text{Re}_2(\text{OOCC}(\text{CH}_3)_3)_4\text{Cl}_2\}^-$ and a significant spin density on the cobalt atoms (see Table 5). This explanation fits well with the measured voltammetric behavior of **2**.

Conclusion

The rhenium trifluoroacetate precursor $\text{N}(\text{C}_4\text{H}_9)_4[\text{Re}_2(\text{OOCCF}_3)_4\text{Cl}_6]$ allows the synthesis of the new polymetallic compound **2**. The cluster carboxylate ligand $(\text{CO})_6\text{Co}_2\text{HCCCOO}$ has been shown to form a μ_2 -bridged rhenium complex which is structurally very similar to the rhenium carboxylates, $\text{Re}_2(\text{OOCR})_4\text{Cl}_2$ (i.e. pivalate). However, the electronic structure of **2** is different from that of “simple” carboxylates, as shown by cyclic voltammetric data. Upon reduction, the cluster-carbonyl fragment in **2** acts as an “electron buffer”, delocalizing the additional charge, as shown by the DFT results.

Acknowledgment. The authors acknowledge financial support of the FONDECYT (Grants 1980896, 2990093, and 4000027), FONDAP (Grant 11980002), and CNRS/CONICYT French/Chilean cooperation project PICS 922.

Note Added after ASAP: Due to a production error, an uncorrected version of this paper was inadvertently posted ASAP on September 26, 2002. The correct version was posted on October 4, 2002.

Supporting Information Available: X-ray data in CIF format for $\text{Re}_2(\mu_2\text{-Cl})_2(\text{CO})_8$, **1**, and **2** and cyclic voltamogram and thermogravimetric analysis figures for **2**. This material is available free of charge via the Internet at <http://pubs.acs.org>.

IC020234E